Extremophiles (2007) 11:159–168
DOI 10.1007/s00792-006-0029-y

ORIGINAL PAPER

Mark Dopson · Craig Baker-Austin · Philip Bond

Towards determining details of anaerobic growth coupled to ferric iron reduction by the acidophilic archaeon '*Ferroplasma acidarmanus*' Fer1

Received: 11 July 2006 / Accepted: 19 July 2006 / Published online: 18 October 2006

Abstract Elucidation of the different growth states of *Ferroplasma* species is crucial in understanding the cycling of iron in acid leaching sites. Therefore, a proteomic and biochemical study of anaerobic growth in '*Ferroplasma acidarmanus*' Fer1 has been carried out. Anaerobic growth in *Ferroplasma* spp. occurred by coupling oxidation of organic carbon with the reduction of Fe^{3+}; but sulfate, nitrate, sulfite, thiosulfate, and arsenate were not utilized as electron acceptors. Rates of Fe^{3+} reduction were similar to other acidophilic chemoorganotrophs. Analysis of the '*F. acidarmanus*' Fer1 proteome by 2-dimensional polyacrylamide gel electrophoresis revealed ten key proteins linked with central metabolic pathways ≥4 fold up-regulated during anaerobic growth. These included proteins putatively identified as associated with the reductive tricarboxylic acid pathway used for anaerobic energy production, and others including a putative flavoprotein involved in electron transport. Inhibition of anaerobic growth and Fe^{3+} reduction by inhibitors suggests the involvement of electron transport in Fe^{3+} reduction. This study has increased the knowledge of anaerobic growth in this biotechnologically and environmentally important acidophilic archaeon.

Keywords Ferroplasma · Proteomics · Anaerobic · Electron transport · Metabolism

Abbreviations

AMD	Acid mine drainage
S^0	Elemental sulfur
RISC	Reduced inorganic sulfur compound
MSM	Mineral salts medium
2D-PAGE	2-Dimensional polyacrylamide gel electrophoresis
MALDI-TOF	Matrix-assisted laser desorption ionization time-of-flight
1D-PAGE	1-Dimensional polyacrylamide gel electrophoresis
TCA	Tricarboxylic acid
HQNO	2-Heptyl-4-Hydroxyquinoline *N*-oxide

Introduction

Strains from the genus *Ferroplasma* have been isolated from one of the most acidic, metal rich natural environments known (Nordstrom et al. 2000) as well as from biooxidation tanks for the recovery of metals from ores (Edwards et al. 2000; Okibe et al. 2003; Dopson et al. 2004b). Physiological and ecological aspects of the extreme acidophiles *Ferroplasma* are recently reviewed in Golyshina and Timmis (2005). *Ferroplasma* spp. are of interest from both environmental and biotechnological perspectives, partly because of their role as intermediates in biogeochemical cycling (Dopson et al. 2003), but also because of their extremely low optimal growth pH (Dopson et al. 2004b), role in acid mine drainage (AMD) production, as well as remarkable resistance to a range of heavy metals (Dopson et al. 2003; Baker-Austin et al. 2005). *Ferroplasma* isolates have been characterized as constituting two species, *Ferroplasma acidiphilum*

Communicated by G. Antranikian.

M. Dopson · C. Baker-Austin · P. Bond
School of Biological Sciences, University of East Anglia, Norwich NR4 7TJ, UK

M. Dopson
Molecular Biology, Umeå University, 901 87 Umea, Sweden

P. Bond
Centre for Ecology, Evolution and Conservation, University of East Anglia, Norwich NR4 7TJ, UK

Present address: P. Bond (✉)
Advanced Wastewater Management Centre, University of Queensland, Queensland 4072, Australia
E-mail: phil.bond@awmc.uq.edu.au

Present address: C. Baker-Austin
Savannah River Ecology Laboratory, University of Georgia, Aiken, SC, USA

and '*Ferroplasma acidarmanus*' (Edwards et al. 2000; Golyshina et al. 2000; Dopson et al. 2004b). The genomes of two *Ferroplasma* strains have been sequenced; '*F. acidarmanus*' Fer1 (97% complete; draft results at: http://www.genome.ornl.gov/microbial/faci/) and *Ferroplasma* Type II (Tyson et al. 2004). In neither of the results from genome sequencing has a putative anaerobic growth mechanism or pathway been hypothesized.

Acidic environments are known to contain anoxic zones, including AMD sites and sulfide mineral heap leaching operations due to variations in permeability to gases, oxidation rates, sulfide–sulfur content, water inundation, and bacterial populations (reviewed in Brierley 2001). Alternating aerobic/anaerobic respiration would be an important characteristic to enable survival and proliferation in these environments. Acidophilic microorganisms catalyze the dissolution of sulfide minerals that may result in the accumulation of Fe^{3+}, arsenate (AsO_4^{3-}), elemental sulfur (S^0), reduced inorganic sulfur compounds (RISC's), and sulfate (Suzuki 2001). In some sites the concentration of Fe^{3+} may reach several orders of magnitude greater than molecular oxygen, and along with S^0, sulfate, and AsO_4^{3-}, these serve as electron acceptors for acidophilic facultative anaerobes such as *Acidithiobacillus ferrooxidans* (Hallberg et al. 2001; Ohmura et al. 2002), *Acidiphilium* spp. (Kusel et al. 1999; Johnson and Bridge 2002), and *Sulfobacillus* spp. (Johnson and McGinness 1991; Bridge and Johnson 1998). The redox couple of Fe^{2+}/Fe^{3+} (+770 mV at pH 2) allows the coupling of H_2, S^0, RISC's, or organic compounds to Fe^{3+} reduction. Although anaerobic growth by these bacterial species has been demonstrated, the genetic and biochemical mechanisms of archaeal Fe^{3+} reduction have not been elucidated.

Recently we reported anaerobic growth of *Ferroplasma* spp. via yeast extract/Fe^{3+} (Dopson et al. 2004b). In this paper we have utilized proteomic, membrane spectra, and electron transport inhibitor studies to further investigate anaerobic chemoorganotrophic growth by *Ferroplasma* spp.

Experimental procedures

Strains and batch growth conditions

The *Ferroplasma* strains used were '*F. acidarmanus*' Fer1 (Edwards et al. 2000) and *F. acidiphilum* Y^T (DSM 12658; Golyshina et al. 2000). Both species were initially grown in batch culture (Dopson et al. 2004b). For measurement of anaerobic growth, Hungate tubes and conical flasks (10 and 50 ml total volumes, respectively) with suba-seals were prepared in triplicate containing mineral salts medium (MSM) pH 1.2 plus trace elements (Dopson et al. 2004b), and inhibitors as required. Where appropriate, $FeSO_4$ and $Fe_2(SO_4)_3$ were added as electron donor and acceptor, respectively. The trace elements (100 × stock solution) were prepared in ultrapure water and adjusted to pH 1.6. The 10% (wt/vol) yeast extract (500 × stock solution for 0.02% (wt/vol) final concentration) was prepared in ultrapure water. MSM contains a total of 28 mM sulfate (from ammonium, sodium, and magnesium salts; not including the trace element solution) plus 62.5 mM from H_2SO_4 addition to adjust the pH to 1.2, giving a total of 90.5 mM sulfate. Both Hungate tubes and conical flasks were sparged for > 30 min with N_2 to remove oxygen and where indicated inoculated with *Ferroplasma* cells equivalent to 10 μg protein per tube or flask. The inoculum was prepared from glass gas-lift continuous culture vessels maintained in steady state anaerobic growth (see below). Prior to inoculation, cells were washed in MSM to remove any Fe^{3+} carried over from the continuous culture vessel. *Ferroplasma* spp. in Hungate tubes were placed in a gas jar to completely ensure they were anaerobic (the atmosphere inside the gas jars was CO_2) and grown stationary for 22 days at 37°C. Growth was analyzed by measurement of whole cell protein concentration using the Bio-Rad "Protein Assay Dye Reagent Concentrate" which was chosen as it was not affected by acidic pH. Protein analysis was carried out by centrifugation of the cells at 10,000*g* for 30 min and removal of the supernatant. The cell pellet was re-suspended in 200 μl assay reagent that contains phosphoric acid and methanol and incubated at room temperature for 5 min to lyse the cells. The protein assay dye was diluted with 800 μl ultrapure water and incubated at room temperature for 30 min for color development. Protein concentration with bovine serum albumin as standard was analyzed according to the manufacturer's instructions. A standard curve of cell number versus protein concentration was generated and showed that they increased proportionally (data not shown). Conical flasks were incubated by shaking at 37°C and sampled through the suba-seal using a needle whilst sparging the head space with N_2. Samples were analyzed for protein concentration (as above), total and ferrous iron determined using ferrozine as the indicator (Dawson and Lyle 1990) or cerium sulfate (Kolthoff and Sandell 1963) as described in Dopson and Lindström (1999) with means (number of replicates, $n = 3$) ± SD presented.

Growth in continuous culture

Initially, '*F. acidarmanus*' Fer1 was grown chemomixotrophically under aerobic conditions in a 1.5 l continuous culture vessel on MSM plus $FeSO_4$ (as above). When steady state growth was reached (with a medium flow rate of $D = 0.01\ h^{-1}$) the airflow was steadily decreased in the vessel over a 10 day period before being shut off and replaced by 800 ml $N_2\ min^{-1}$. When the gas flow was switched to N_2, the feed to the continuous culture vessel was replaced with MSM containing trace elements, 0.02% (wt/vol) yeast extract, and 10 mM $Fe_2(SO_4)_3$ (this time point was designated 0 culture volumes). The continuous culture vessel was regularly

sampled and the medium flow rate decreased to $D = 0.005\ h^{-1}$ until steady state was reached as determined by monitoring protein, total iron, and Fe^{2+} concentrations (as above). During steady state growth, cells were harvested for 2-dimensional polyacrylamide gel electrophoresis (2D-PAGE). The theoretical washout rate (Pritchard and Tempest 1982) was calculated as described in Dopson et al. (2005).

Electron microscopy

Transmission electron micrographs were taken of '*F. acidarmanus*' Fer1 whole cells grown aerobically and anaerobically in continuous culture vessels (Dopson et al. 2004b). The Fe crystals were identified by X-ray diffraction.

2D-PAGE, protein excision, and analysis

2D-PAGE analysis was carried out according to Dopson et al. (2004a) that was adapted from Hesketh et al. (2002). Protein expression, spot matching, spot presence or absence, and statistics from the 2D-PAGE gels were analyzed using ProteomWeaver version 1.3 (Definiens) and composite gels produced from replicates ($n = 2$). ProteomWeaver normalizes protein spot density based on the entire protein complement on the gels and therefore, the intensity of individual spots is adjusted on the basis of the total protein detected on the gels. This alleviates the need for internal protein standards and adjusts for small differences in protein loading and gel development. Identification of matrix-assisted laser desorption ionization time-of-flight (MALDI-TOF) mass spectrometry peptide mass fingerprint data was carried out using MASCOT against theoretical MALDI-TOF mass fingerprints calculated from the '*F. acidarmanus*' Fer1 sequence database. The MOWSE score cut off point for >95% confidence that the protein match was not a random event was calculated by MASCOT to be 41. The parameters used during the MASCOT search were carbamidomethyl (fixed modifications) and oxidation (variable modifications), ±50 ppm peptide mass tolerance, and a maximum of one missed cleavage. Putative protein identification and function were deduced from the genome analysis (http://www.genome.ornl.gov/microbial/faci/).

Extraction and analysis of membrane proteins

Membrane fractions were isolated, separated, and analyzed on a 1-dimensional protein gel (1D-PAGE; Dopson et al. 2005). Proteins were stained with either coomassie or haem stain (Thomas et al. 1976). Differentially expressed bands were excised and identified by mass spectrometry (as described above). UV-visible spectra of membrane proteins were acquired using a Hitachi U4001 UV-visible spectrophotometer (Dopson et al. 2005).

Direct assay of ferric reduction

Fe^{3+} reduction was assayed by measuring the increase in Fe^{2+} production in Hungate tubes (10 ml total volume) containing MSM, substrate (as indicated), 80 μmol $Fe_2(SO_4)_3$, and indicated electron transport chain inhibitors. The tubes were sparged with N_2 (>30 min) and the reaction started by addition of cell mass equivalent to between 451 and 792 μg cell protein. Samples (100 μl) were removed at the indicated times and Fe^{2+} production measured using ferrozine (Dawson and Lyle 1990). Results were calculated as the increase of Fe^{2+} (μmol), minus the Fe^{2+} concentration at the start of the respective experiment, and presented (means of triplicate experiments ± SD) as μmol Fe^{2+} produced mg protein^{-1}.

Results and discussion

Very little is known concerning the biochemistry of dissimilatory iron reduction, despite it being thought to be one of the oldest energy-generating processes (Richardson 2000). At neutral pH, dissimilatory iron reduction generally utilizes an insoluble electron acceptor (Fe^{3+} solubility decreases rapidly above pH 1.6) and the pre-dominant proteins involved in electron transfer to Fe^{3+} are *c*-type cytochromes (reviewed in Schröder et al. 2003).

Anaerobic growth and Fe^{3+} reduction in batch experiments

'*F. acidarmanus*' Fer1 anaerobic growth utilizing 0.02% (wt/vol) yeast extract and Fe^{3+} as electron donor and acceptor, respectively, was observed (Fig. 1a). No production of Fe^{2+} from Fe^{3+} was measured in cell free controls with 0.02% (wt/vol) yeast extract, suggesting that Fe^{3+} reduction was not abiotic (data not shown). A lag phase of 162 h occurred during which Fe^{3+} reduction was minimal. After this time, exponential growth was observed with a generation time of 43.5 h and a concomitant increase in the rate of Fe^{3+} reduction. After 259 h, peak protein concentration was reached at 6.3 mg protein l^{-1} although Fe^{3+} reduction continued until 406 h. A total of 7.0 ± 1.2 mM Fe^{3+} was reduced from the available 9.7 ± 0.1 mM at the start of the experiment (Fig. 1b). The generation time for anaerobic growth via Fe^{3+} reduction by *Acidiphilium acidophilum* was estimated from data by Johnson and Bridge (2002) to be approximately 33 h, giving a slightly higher growth rate than that for '*F. acidarmanus*' Fer1. Although the generation time was shorter for *A. acidophilum*, the rate

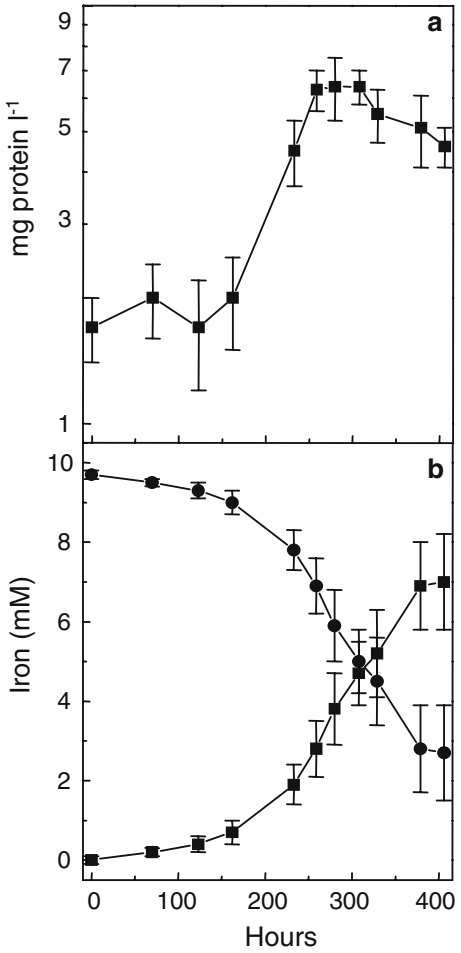

Fig. 1 Semi-log plot of '*F. acidarmanus*' Fer1 anaerobic growth (*filled square*) on 0.02% yeast extract and 10 mM Fe^{3+} measured as protein concentration (**a**). Reduction in Fe^{3+} concentration (*filled circle*) and the concomitant increase in Fe^{2+} (*filled square*) are shown (**b**). Values are means ± SD (n = 3)

of Fe^{3+} reduction by '*F. acidarmanus*' Fer1 was similar to that by washed cell suspensions of *Acidiphilium* SJH and *A. acidophilum* (Johnson and Bridge 2002). As the Hungate tubes and shake flasks were sparged with N_2 for 30 min it is possible that Fe^{3+} reduction was initiated in the presence of low concentrations of oxygen, as has been observed for *A. cryptum* (Kusel et al. 2002). That Fe^{3+} reduction continued after total protein stopped increasing may be due to a lack of an essential nutrient halting balanced growth, but allowing Fe^{3+} reduction to continue. Alternatively, simultaneous cell death and growth may have occurred. This possibility is supported by the decrease in protein concentration at the end of growth.

Identification of electron donors and acceptors

Potential electron donors and acceptors for anaerobic growth by *Ferroplasma* spp. were tested in Hungate tubes (Table 1). Controls containing Fe^{2+} were established to show that no aerobic growth occurred. Also, no growth occurred with yeast extract without $Fe_2(SO_4)_3$ as electron acceptor, suggesting that neither fermentation or sulfate reduction occurred (MSM contains 90.5 mM SO_4^{2-}). Both *Ferroplasma* spp. could grow on yeast extract whilst reducing Fe^{3+}. The *Ferroplasma* species grew to a higher protein concentration on different concentrations of yeast extract (0.04% for '*F. acidarmanus*' Fer1 and 0.02% for *F. acidiphilum* Y^T) suggesting different growth requirements for, and perhaps tolerance to, organic carbon. Similar organic carbon requirements have been observed for '*F. acidarmanus*' Fer1 aerobic chemomixotrophic growth (Dopson et al. 2005). The reported protein concentrations were lower in Table 1 compared to Fig. 1 due to the conical flasks were incubated shaken ensuring homogenous distribution of electron donors and higher growth rates. A very low level of growth was observed by *F. acidiphilum* Y^T with the electron donor/acceptor combination yeast extract/S^0; although no H_2S formation was detected by color change or odor. Other electron donor/acceptor combinations that did not support anaerobic growth for either *Ferroplasma* species were yeast extract/NO_3^-, yeast extract/SO_3^{2-}, yeast extract/$S_2O_3^{2-}$, yeast extract/AsO_4^{3-}, and formate/Fe^{3+} (data not shown).

Anaerobic growth in continuous culture

Steady state protein concentration was reached after 2.2 culture volumes, although the total Fe may still have been increasing. During the time that the protein concentration was in steady state nine samples were removed over a period of 15 days (corresponding to 1.9 culture volumes) giving an average protein concentration of 3.8 ± 0.4 mg protein l^{-1} (n = 9; Fig. 2a). The amount of protein in the anaerobic continuous culture was lower than the maximum concentration observed during aerobic chemomixotrophic continuous culture growth of 25.7 mg protein l^{-1} (Dopson, un-published). During anaerobic growth, the total iron increased from 9.1 ± 0.9 mM at 0.83 culture volumes to 13.4 ± 0.5 mM (n = 9) after 3.26 culture volumes (averages ± SD were calculated as for steady state protein concentration; Fig. 2b). During the same period the Fe^{2+} concentration increased from 2.5 ± 0.1 mM to a steady state of 6.2 ± 0.2 mM (n = 15) after 2.77 culture volumes, indicating that Fe^{3+} reduction was occurring. The total iron in the continuous culture vessel during steady state protein concentration was greater than the concentration in the feed (10 mM Fe^{3+}) and therefore, iron must have been accumulating within the vessel. Electron micrographs showed deposits on the surface of '*F. acidarmanus*' Fer1 when grown anaerobically (Fig. 3a) that were not present during aerobic chemomixotrophic growth in continuous culture vessels (Fig. 3b). The deposits were analyzed by X-ray diffraction and identified as iron, possibly in the form of magnetite which characteristically accumulates on the

Table 1 Anaerobic growth (detected as the increase in protein concentration) of '*F. acidarmanus*' Fer1 and *F. acididphilum* Y^T following incubation for 22 days at 37°C in Hungate tubes in the presence of various electron donors and acceptors

Electron donor	Added electron acceptor	'*F. acidarmanus*' Fer1 (mg protein l^{-1a})	*F. acididphilum* Y^T (mg protein l^{-1a})
Fe^{2+} control	None	NG	NG
0.02% Yeast extract	None (SO_4^{2-}; control)[b]	NG	NG
0.02% Yeast extract	10 mM Fe^{3+}	1.8 ± 0.5	2.1 ± 0.9
0.04% Yeast extract	10 mM Fe^{3+}	3.1 ± 1.1	0.5 ± 0.3
10 mM Glucose	10 mM Fe^{3+}	1.1 ± 0.6	0.7 ± 0.2
10 mM Glycerol	10 mM Fe^{3+}	0.5 ± 0.4	0.6 ± 0.3
10 mM Acetate	10 mM Fe^{3+}	0.7 ± 0.4	NG
0.02% Yeast extract	10 mM S^0	NG	0.3 ± 0.2

NG no growth detected
[a]Values are means minus the no substrate control ± SD calculated as the square root of the sum of the squares of the SD of the test and no substrate control (both $n = 3$)
[b]MSM contains 90.5 mM SO_4^{2-}

surface of Fe^{3+} respiring prokaryotes (Richardson 2000). The difference in size between anaerobic and aerobic grown '*F. acidarmanus*' Fer1 (Fig. 3) has also been seen for aerobic chemomixotrophic versus chemoheterotrophic growth (Dopson et al. 2004b).

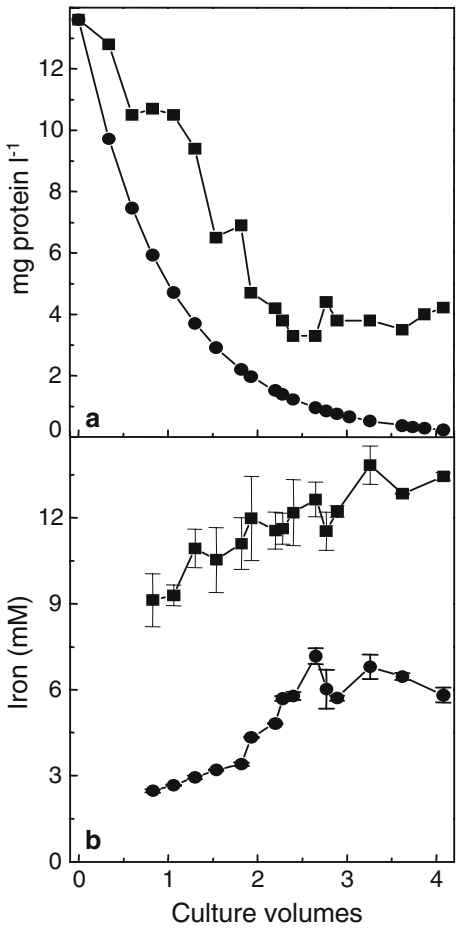

Fig. 2 Anaerobic growth of '*F. acidarmanus*' Fer1 in continuous culture on 0.02% yeast extract and 10 mM Fe^{3+} (**a**) showing protein concentration (*filled square*) and theoretical protein washout rate (*filled circle*). Total iron (*filled square*) and Fe^{2+} (*filled circle*) over the course of the continuous culture experiment are also given (**b**). Data points in **b** are means ± SD ($n = 3$)

Proteomic analysis of anaerobic growth

Aerobic and anaerobic chemoorganotrophic growth utilizing O_2 and Fe^{3+} as electron acceptors, respectively, was carried out in continuous culture vessels and analyzed by 2D-PAGE (Fig. 4). Those protein spots not present during aerobic growth or greater than fourfold up-regulated during anaerobic growth were identified (Table 2).

Proteins identified as up-regulated during anaerobic growth included a putative enolase that is unique to the anaerobic respiration pathway that utilizes organic carbon by way of 2-phosphoglycerate to succinate via the reductive tricarboxylic acid (TCA) cycle (Table 2). A further identified protein was subunit A of succinate dehydrogenase/fumarate reductase. Succinate dehydrogenase passes electrons to the ubiquinone and the ubiquinol formed reduces the bc_1 complex in the reverse TCA pathway during anaerobic respiration, whereas fumarate reductase acts as a terminal reductase during fermentation (Cecchini et al. 2002). Succinate dehydrogenase and fumarate reductase cannot be functionally distinguished on the basis of DNA sequence and therefore, further identification based on proteomics is not possible. However, '*F. acidarmanus*' Fer1 contains a cytochrome *b* related protein (QcrB homologue) contained in the bc_1 complex that is an ubiquinol cytochrome *c* reductase suggesting that the identified protein in the proteomics is succinate dehydrogenase. A further gene in the electron transport chain, detected as 6.4 fold up-regulated, was a putative Rieske iron-sulfur protein most similar to SoxF from *Sulfolobus* spp. that acts with SoxEG to form a complex with an analogous function to bc_1/b_6f complexes (Komorowski et al. 2002). The other enzymes in the reverse TCA pathway are also utilized during aerobic chemoorganotrophic growth and therefore would not necessarily be expected to be identified as up-regulated. A putative electron transfer flavoprotein required for anaerobic carnitine metabolism (Walt and Kahn 2002) was also up-regulated under anaerobic conditions. An alternative anaerobic pathway down-

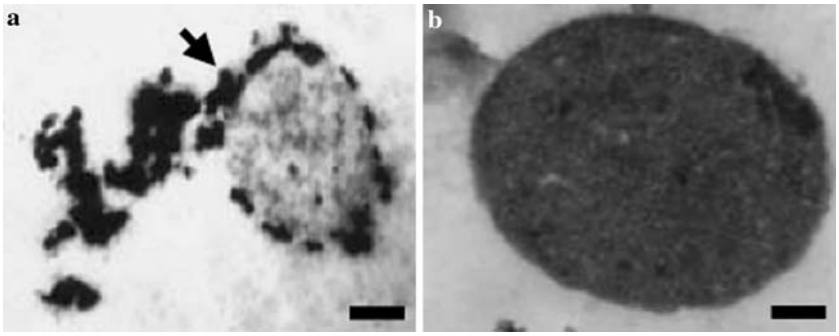

Fig. 3 Transmission electron micrographs of '*F. acidarmanus*' Fer1 during anaerobic (Fe^{3+} electron acceptor) chemoorganotrophic growth (**a**), and aerobic (O_2 electron acceptor) chemomixotrophic growth (**b**), taken from continuous culture vessels. During anaerobic growth iron accumulated on the cell surface (indicated by *arrow*). *Scale bars*; 200 nm

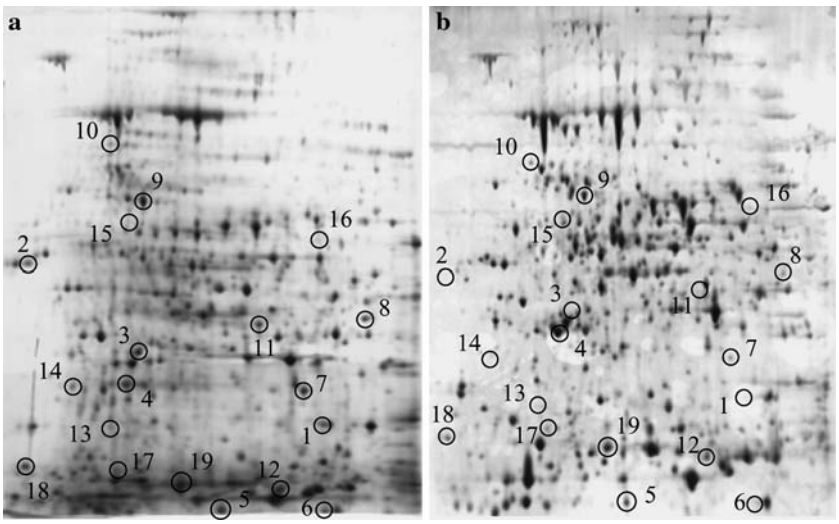

Fig. 4 2D-PAGE gels of whole cell protein from '*F. acidarmanus*' Fer1 grown anaerobically on 0.02% yeast extract + 10 mM Fe^{3+} (**a**) and aerobically on 0.02% yeast extract (**b**). Spots analyzed by MALDI-TOF mass spectrometry are labeled (spot numbers correspond to Table 2) on the anaerobic gel and corresponding aerobic spots are also *circled*. Apparent differences in spot intensity may not precisely match those listed in the tables (regulation), as the latter were derived by comparison of composite images (not shown) prepared from replicate gels

stream of the phosphoenolpyruvate produced by enolase (with one reaction in between) is the conversion of pyruvate to acetyl CoA by pyruvate dehydrogenase and its reverse reaction by pyruvate ferredoxin oxidoreductase during fermentation. The product of the up-regulated protein 2-keto-3-deoxy gluconate aldolase is pyruvate that may also feed into the above reaction pathway. The acetyl CoA can be converted to acetaldehyde and then to ethanol by the up-regulated aldo/keto reductase enzyme family protein (putatively alcohol dehydrogenase).

Proteins with high similarity to the α- and β-subunits of pyruvate dehydrogenase were also up-regulated. In addition, proteins with high similarity to α and β subunits of pyruvate ferredoxin oxidoreductase were only detected under anaerobic conditions. Proteins of this type are grouped as general oxoacid:ferredoxin oxidoreductases (Huynen et al. 1999), and one possible reaction of this group under anaerobic conditions is to decarboxylate pyruvate to acetyl CoA. This latter reaction is reversible and it is possible that pyruvate dehydrogenase and pyruvate ferredoxin oxidoreductase may be used to control metabolic flux by regulating acetyl CoA and pyruvate concentrations. Also feeding into anaerobic metabolic pathways could be the product of 2-keto-3-deoxy gluconate aldolase, an enzyme involved in glucose metabolism that produces pyruvate and glyceraldehyde-3-phosphate. A protein with high similarity to a Fe-S oxidoreductase was also up-regulated.

A RNA polymerase subunit (*rpoA* gene) homologue was also up-regulated (Table 2). Mutations in the *Salmonella typhimurium rpoA* have been shown to affect expression of anaerobically regulated genes (Lombardo et al. 1991). *rpoA* has been suggested to interact with the redox-responsive transcriptional regulator fumarate nitrate reductase regulator (FNR; although no homologue has been identified on the '*F. acidarmanus*' Fer1 genome) that activates or represses the expression of a family of genes concerned with anaerobic metabolism (Lombardo et al. 1991). Two proteins with homology to stress proteins were also up-regulated (Table 2). These were a DNA helicase induced by DNA damage, possibly in response to damage caused by the presence of free, unsequestered cytoplasmic iron (reviewed in Andrews et al. 2003) and a protein with homology to GroEL that has an essential role in mediating protein folding.

Spectrophotometric analysis of respiratory proteins

The oxidized peak in the anaerobic chemoorganotrophic membranes from approximately 415 to 455 nm (Fig. 5) is due to the Soret band and may be made up of a combination of cytochromes *b* and *c* (Komorowski et al.

Table 2 Identification of '*F. acidarmanus*' Fer1 proteins induced under anaerobic conditions from 1D and 2D-PAGE gels

Fer1 gene[a]	Putative protein function	Regulation[b]	MOWSE[c]	e-value and organism[d]	Coverage[e]	Ave ± SD[f]	Motif(s)[g]
Metabolic and electron transport proteins							
164.1059[1]	Succinate dehydrogenase/fumarate reductase (subunit A)	NP[h]	140	0 (*Acidianus ambivalens*)	24	0.69 ± 0.03	TIGR sdhA_frdA_Gneg, & COG 1053
162.916[2]	Pyruvate dehydrogenase complex (α sub-unit)	NP	174	$7e^{-53}$ (*T. volcanium*)	37	0.54 ± 0.01	PFam E1_dh & COG 1071
162.917[3]	Pyruvate dehydrogenase complex (β sub-unit)	NP	189	$1e^{-128}$ (*T. volcanium*)	61	0.52 ± 0.45	Pfam Transket_pyr & COG 0022
160.767[4]	Pyruvate ferredoxin oxidoreductase (β sub-unit)	NP	159	$1e^{-112}$ (*T. volcanium*)	48	1.02 ± 0.33	PFam TPP_enzyme_C & COG 1013
164.1018	Pyruvate ferredoxin oxidoreductase (α sub-unit)	NP	151	$2e^{-83}$ (*T. volcanium*)	35	NA[x]	PFam POR_N & COG 0674
166.1219	Electron transfer flavoprotein (α sub-unit)	NP	72	0 (*Sulfolobus tokodaii*)	23	NA	PFam ETF_alpha & COG 2025
164.1067[5]	2-keto-3-deoxy gluconate aldolase	124.4	68	$3e^{-62}$ (*T. volcanium*)	20	1.38 ± 0.07	PFam DHDPS & COG 0329
168.1529[6]	Aminomethyltransferase (GcvT)	25.7	53	$1e^{-124}$ (*T. volcanium*)	10	1.53 ± 0.64	PFam GCV_T, TIGR gcvT, & COG 0404
126.50[7]	Aldo/keto reductase family	24.2	100	$3e^{-73}$ (*S. solfataricus*)	67	1.15 ± 0.09	PFam Aldo_ket_red & COG 0656
147.216[8]	Rieske iron-sulfur protein SoxF (QcrA)	6.4	48	$2e^{-25}$ (*T. acidophilum*)	20	0.62 ± 0.01	COG 0723
159.681[9]	Enolase (Eno)	5.4	81	$1e^{-148}$ (*T. volcanium*)	24	1.31 ± 0.21	PFam Enolase_C & COG 0148
157.545	Fe-S oxidoreductase	4.4	93	0 (*T. volcanium*)	25	NA	PFam Radical_SAM & COG 1032
Biosynthetic proteins							
146.207[10]	Glutamine synthetase (GlnA)	10.5	46	$1e^{-163}$ (*T. volcanium*)	14	0.25 ± 0.09	PFam Gln-synt_C, TIGR GlnA, & COG 0174
Transcription and translation components							
163.981[11]	Initiation factor 2 subunit family	NP	234	$1e^{-143}$ (*T. volcanium*)	49	0.63 ± 0.06	PFam IF-2B, TIGR eIF-2B_rel, & COG 0182
168.1488[12]	RNA-binding protein Rrp4 - exoribonuclease	62.4	73	$5e^{-75}$ (*T. volcanium*)	31	0.95 ± 0.23	PFam KH_1 & COG 1097
168.1490[13]	RNase exoribonuclease	7.1	158	$1e^{-92}$ (*T. volcanium*)	37	0.24 ± 0.10	PFam RNase_PH & COG 2123
156.484[14]	RNA polymerase subunit D (RpoA)	6.6	43	$1e^{-103}$ (*T. volcanium*)	15	0.12 ± 0.09	PFam RNA_pol_A_bac & COG 0202
169.1602[15]	30S Ribosomal protein S24e	5.1	58	$2e^{-23}$ (*T. volcanium*)	30	0.12 ± 0.14	PFam Ribosomal_S24e & COG 2004
Stress proteins and chaperones							
157.581[16]	DNA helicase (DinG)	5.5	42	$8e^{-57}$ (*S. solfataricus*)	8	0.09 ± 0.05	PFam DEAD_2 & COG 1199
165.1085[15]	Thermosome β subunit (HSP60 family)	5.1	58	0 (*T. acidophilum*)	9	0.12 ± 0.14	PFam Cpn60_TCP1 & COG 0459
Proteases							
167.1369[17]	20S proteasome α subunit (Pre1)	7.5	126	$2e^{-95}$ (*T. volcanium*)	55	0.35 ± 0.02	PFam Proteasome & COG 0638
169.1624	Proline dipeptidase	4.0	45	$1e^{-119}$ (*T. volcanium*)	28	NA	PFam Peptidase_M24 & COG 0006
Other proteins							
164.1050[18]	Hypothetical protein (*Thermoplasma volcanium*)	12.9	228	$1e^{-53}$ (*T. volcanium*)	68	1.53 ± 0.73	PFam TPR & COG 3063
166.1225[19]	Hypothetical protein (*S. tokodaii*)	6.1	158	$2e^{-40}$ (*S. tokodaii*)	59	2.84 ± 1.70	COG0715

[a]Designates the contig and gene numbers for the protein as identified on the '*F. acidarmanus*' Fer1 draft genome analysis (http://www.genome.ornl.gov/microbial/faci/). Numbers correspond to the labeled spots on Fig. 4. Those contig and gene numbers without a spot label were identified from the 1D-PAGE gel of membrane proteins

[b]Regulation refers to the increase in protein expression determined by comparison of gel sets using ProteomWeaver (see Experimental procedures)

[c]MOWSE peptide matching score

[d]e-value from the BLAST score (Altschul et al. 1997) for the putative protein taken from the '*F. acidarmanus*' Fer1 draft genome analysis (http://www.genome.ornl.gov/microbial/faci/)

[e]Percentage of the total amino acids identified by MALDI-TOF mass spectroscopy

[f]Average ± SD of spot intensity of the replicates calculated by ProteomWeaver

[g]Motif and domains identified in the proteins (taken from (http://www.genome.ornl.gov/microbial/faci/). Pfam, protein families; and TIGR, TIGRfam Model Comparison

[h]NP, designates the spot is not present in the corresponding gel set

[x]NA, Not available

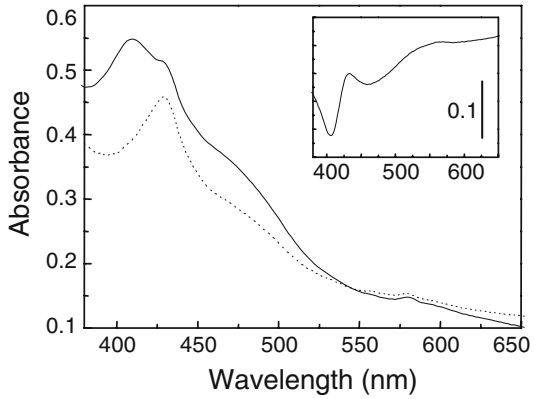

Fig. 5 Air oxidized (*solid line*) and dithionite reduced (*dotted line*) spectra of anaerobic '*F. acidarmanus*' Fer1 membranes. *Inset* is dithionite reduced—air oxidized difference spectra (*scale bar* gives an optical density of 0.1)

Table 3 Anaerobic growth (measured as an increase in protein concentration) of '*F. acidarmanus*' Fer1 on 0.04% YE + 10 mM Fe^{3+} in the presence of electron transport inhibitors

Inhibitor	Point of inhibition	mg protein l^{-1a}
None	None	2.8 ± 0.7
Rotenone (40 μM)	NADH ubiquinone oxidoreductase	0.0 ± 0.3
Quinacrine (1 mM)	Flavoprotein electron transfer	0.7 ± 0.4
Antimycin A (0.5 μM)	bc_1 reductase	0.0 ± 0.4
HQNO (40 μM)	Quinol oxidases and reductases	2.9 ± 0.7
Azide (1 mM)	Cytochrome *c*	0.8 ± 0.1

[a]Values are averages minus the no substrate control ± SD calculated as the square root of the sum of the squares of the SD of the test and control (both $n = 3$)

2002; Brasseur et al. 2004). The absorption in the Soret band has a peak at 418 nm indicating the presence of a cytochrome *c*. A shift in the anaerobic grown membrane preparation optical density of the peak at 423–437 nm also suggests the presence of a haem protein. The peaks in the anaerobic membranes oxidized spectra at 410 (large) and 425 nm (broad) are typical of Fe-S clusters from one or more redox proteins. The flavoprotein peak visible in aerobic grown membranes (Dopson et al. 2005) is not present in anaerobic membranes despite up-regulation of the membrane bound flavoprotein, succinate reductase/fumarate dehydrogenase (Table 2). This apparent contradiction may be explained by a possible overall down-regulation of flavoproteins in the anaerobic grown '*F. acidarmanus*' Fer1, whilst the high resolution of the 2D-PAGE identified the specific up-regulation of succinate reductase/fumarate dehydrogenase. The haem stained 1D-PAGE gel had a single band, corresponding to an approximately 34 kDa protein (data not shown) that was also present in aerobic, chemomixotrophic but not chemoheterotrophic grown membranes (Dopson et al. 2005).

Anaerobic growth and Fe^{3+} reduction by '*F. acidarmanus*' Fer1 in the presence of inhibitors

All of the tested electron transport inhibitors reduced the level of anaerobic growth compared to the control except 2-Heptyl-4-Hydroxyquinoline *N*-oxide (HQNO; Table 3). The point of inhibition for each of the inhibitors are: rotenone is an inhibitor of the NADH ubiquinone oxidoreductase (Degli Esposti 1998); quinacrine is a flavin homolog that competitively inhibits flavoprotein electron transfer as well as inhibiting proteases and hydrogenases; antimycin A non-competitively reduces electron flow through the bacterial bc_1 reductase (Tolkatchev et al. 1996); HQNO inhibits most quinol oxidases and reductases; and azide inhibits cytochrome *c* oxidase as well as nitrate reductase and other enzymes. The reduced growth in the presence of the specific inhibitors rotenone and antimycin A suggests that electron transport was important for anaerobic growth and the other inhibitors may also have affected electron transport.

Fe^{3+} reduction by '*F. acidarmanus*' Fer1 was also determined in resting cells (Table 4). Only small

Table 4 Amount of Fe^{2+} produced from the reduction of Fe^{3+} by '*F. acidarmanus*' Fer1 after 5 h with various electron donors and electron transport inhibitors

'*F. acidarmanus*' Fer1	Electron donor	Inhibitor	μmol Fe^{2+} mg $protein^{-1a}$
No cell control	0.02% yeast extract	None	0.1 ± 0.4
Aerobic grown	0.02% yeast extract	None	0.1 ± 0.4
Anaerobic grown	None	None	0.4 ± 0.1
Anaerobic grown	0.02% yeast extract	None	17.0 ± 0.9
Anaerobic grown	10 mM Glucose	None	15.7 ± 1.5
Anaerobic grown	10 mM Glycerol	None	5.9 ± 0.3
Anaerobic grown	10 mM Acetate	None	5.1 ± 0.7
Anaerobic grown	0.02% yeast extract	Rotenone (40 μM)	1.0 ± 0.4
Anaerobic grown	0.02% yeast extract	Quinacrine (1 mM)	0.1 ± 0.4
Anaerobic grown	0.02% yeast extract	Antimycin A (0.5 μM)	2.0 ± 0.7
Anaerobic grown	0.02% yeast extract	HQNO (40 μM)	7.5 ± 2.0
Anaerobic grown	0.02% yeast extract	Azide (1 mM)	2.1 ± 0.1

[a]Values are averages ± SD ($n = 3$)

amounts of Fe^{3+} reduction was detected in the absence of cells, in the presence of aerobically grown cells, and in the absence of organic carbon substrate. In contrast, anaerobically grown cells in the presence of yeast extract produced 17.0 ± 0.1 μmol Fe^{2+} (n = 3) in 5 h from the reduction of Fe^{3+}. The electron donors that supported growth (Table 1) also resulted in Fe^{3+} reduction. The presence of rotenone, quinacrine, antimycin A, and azide all inhibited the reduction of Fe^{3+}, but HQNO had a much lower effect (Table 4). These results also suggest that electron transport occurred during Fe^{3+} reduction. As whole cells were used in these experiments it cannot be unequivocally stated that these inhibitors did not also cause non-specific inhibitory effects. However, these combined results strongly suggest that '*F. acidarmanus*' Fer1 performs respiration on Fe^{3+} to support anaerobic growth. The up-regulation of the Rieske Fe-S protein (SoxF homolog) and the effect of antimycin A indicate a bc_1 complex homolog acts in anaerobic electron transport. However, no homolog is present on the '*F. acidarmanus*' Fer1 genome, explaining why typical absorption spectra for these proteins were not observed in the membrane spectra. Instead, it has been previously suggested that '*F. acidarmanus*' Fer1 may use a SoxEFG homolog (Tyson et al. 2004; Dopson et al. 2005) with a similar function to bc_1/b_6f complexes (Komorowski et al. 2002) and the results presented here support these previous studies.

Conclusions

In this paper we have demonstrated '*F. acidarmanus*' Fer1 anaerobic growth utilizing organic carbon coupled to Fe^{3+} reduction. The proteomic results suggest that anaerobic growth is mediated by the reductive TCA cycle; and membrane fraction spectra, the haem stained 1D-PAGE gel, and electron transport inhibitor experiments support that Fe^{3+} reduction involves cytochromes *b* and *c*. No results were obtained that suggest either fermentation or sulfate reduction occurred. This study provides the first insights into anaerobic growth by this archaeon.

Acknowledgments We thank JF Banfield and KJ Edwards for provision of '*F. acidarmanus*' Fer1 and helpful discussions. DJ Richardson is acknowledged for assistance in interpreting electron transport data. Trypsin digests and MALDI-TOF analysis of excised proteins was carried out at the John Innes Centre, Norwich. The technical assistance of M Maidment and L Flegg was greatly appreciated and R Evans-Gowing is acknowledged for taking the electron micrographs. This work was funded by a BBSRC Research grant.

References

Altschul SF et al (1997) Gapped BLAST and PSI-BLAST: a new generation of protein database search programs. Nucleic Acids Res 25:3389–3402

Andrews SC, Robinson AK, Rodriguez-Quinones F (2003) Bacterial iron homeostasis. FEMS Microbiol Rev 27:215–237

Baker-Austin C, Dopson M, Wexler M, Sawers G, Bond PL (2005) Molecular insight into extreme copper resistance in the extremophilic archaeon "*Ferroplasma acidarmanus*" Fer1. Microbiology 151:2637–2646

Brasseur G, Levican G, Bonnefoy V, Holmes D, Jedlicki E, Lemesle-Meunier D (2004) Apparent redundancy of electron transfer pathways via bc_1 complexes and terminal oxidases in the extremophilic chemolithoautotrophic *Acidithiobacillus ferrooxidans*. Biochim Biophys Acta 1656:114–126

Bridge TAM, Johnson DB (1998) Reduction of soluble iron and reductive dissolution of ferric iron-containing minerals by moderately thermophilic iron-oxidizing bacteria. Appl Environ Microbiol 64:2181–2186

Brierley CL (2001) Bacterial succession in bioheap leaching. Hydrometallurgy 59:249–255

Cecchini G, Schroder I, Gunsalus RP, Maklashina E (2002) Succinate dehydrogenase and fumarate reductase from *Escherichia coli*. Biochim Biophys Acta Bioenerg 1553:140–157

Dawson MV, Lyle SJ (1990) Spectrophotometric determination of iron and cobalt with ferrozine and dithizone. Talanta 37:1189–1191

Degli Esposti M (1998) Inhibitors of NADH-ubiquinone reductase: an overview. Biochim Biophys Acta Bioenerg 1364:222–235

Dopson M, Baker-Austin C, Bond PL (2004a) First use of 2-dimensional polyacrylamide gel electrophoresis to determine phylogenetic relationships. J Microbiol Methods 58:297–302

Dopson M, Baker-Austin C, Bond PL (2005) Analysis of differential protein expression during growth states of *Ferroplasma* strains and insights into electron transport for iron oxidation. Microbiology 151:4127–4137

Dopson M, Baker-Austin C, Hind A, Bowman JP, Bond PL (2004b) Characterization of *Ferroplasma* isolates and *Ferroplasma acidarmanus* sp. nov., extreme acidophiles from acid mine drainage and industrial bioleaching environments. Appl Environ Microbiol 70:2079–2088

Dopson M, Baker-Austin C, Koppineedi PR, Bond PL (2003) Growth in sulfidic mineral environments: metal resistance mechanisms in acidophilic micro-organisms. Microbiology 149:1959–1970

Dopson M, Lindström EB (1999) Potential role of *Thiobacillus caldus* in arsenopyrite bioleaching. Appl Environ Microbiol 65:36–40

Edwards KJ, Bond PL, Gihring TM, Banfield JF (2000) An archaeal iron-oxidizing extreme acidophile important in acid mine drainage. Science 287:1796–1799

Golyshina OV et al (2000) *Ferroplasma acidiphilum* gen. nov., sp. nov., an acidophilic, autotrophic, ferrous-iron-oxidizing, cell-wall-lacking, mesophilic member of the *Ferroplasmaceae* fam. nov., comprising a distinct lineage of the Archaea. Int J Syst Evol Microbiol 50:997–1006

Golyshina OV, Timmis KN (2005) *Ferroplasma* and relatives, recently discovered cell wall-lacking archaea making a living in extremely acid, heavy metal-rich environments. Environ Microbiol 7:1277–1288

Hallberg KB, Thomson HEC, Boeselt I, Johnson DB (2001) Aerobic and anaerobic sulfur metabolism by acidophilic bacteria. In: Ciminelli VST, Garcia O Jr (eds) International biohydrometallurgy symposium. Elselvier, Ouro Preto, Brazil, pp 423–431

Hesketh A et al (2002) The GlnD and GlnK homologues of *Streptomyces coelicolor* A3(2) are functionally dissimilar to their nitrogen regulatory system counterparts from enteric bacteria. Mol Microbiol 46:319–330

Huynen MA, Dandekar T, Bork P (1999) Variation and evolution of the citric-acid cycle: a genomic perspective. Trends Microbiol 7:281–291

Johnson DB, Bridge TAM (2002) Reduction of ferric iron by acidophilic heterotrophic bacteria: evidence for constitutive and inducible enzyme systems in *Acidiphilium* spp. J Appl Microbiol 92:315–321

Johnson DB, McGinness S (1991) Ferric iron reduction by acidophilic heterotrophic bacteria. Appl Environ Microbiol 57:207–211

Kolthoff JM, Sandell EB (1963) Textbook of quantitative inorganic chemistry. MacMillan Publishing Co., New York

Komorowski L, Verheyen W, Schafer G (2002) The archaeal respiratory supercomplex SoxM from *S. acidocaldarius* combines features of quinole and cytochrome *c* oxidases. Biol Chem 383:1791–1799

Kusel K, Dorsch T, Acker G, Stackebrandt E (1999) Microbial reduction of Fe(III) in acidic sediments: isolation of *Acidiphilium cryptum* JF-5 capable of coupling the reduction of Fe(III) to the oxidation of glucose. Appl Environ Microbiol 65:3633–3640

Kusel K, Roth U, Drake HL (2002) Microbial reduction of Fe(III) in the presence of oxygen under low pH conditions. Environ Microbiol 4:414–421

Lombardo MJ, Bagga D, Miller CG (1991) Mutations in *rpoA* affect expression of anaerobically regulated genes in *Salmonella typhimurium*. J Bacteriol 173:7511–7518

Nordstrom DK, Alpers CN, Ptacek CJ, Blowes DW (2000) Negative pH and extremely acidic mine waters from Iron Mountain, California. Environ Sci Technol 34:254–258

Ohmura N, Sasaki K, Matsumoto N, Saiki H (2002) Anaerobic respiration using Fe^{3+}, S^0, and H_2 in the chemolithoautotrophic bacterium *Acidithiobacillus ferrooxidans*. J Bacteriol 184:2081–2087

Okibe N, Gericke M, Hallberg KB, Johnson DB (2003) Enumeration and characterization of acidophilic microorganisms isolated from a pilot plant stirred-tank bioleaching operation. Appl Environ Microbiol 69:1936–1943

Pritchard RH, Tempest DW (1982) Growth: cells and populations. In: Mandelstam J, McQuillen K, Dawes I (eds) Biochemistry of bacterial growth, 3rd edn. Blackwell Scientific Publications, Oxford

Richardson DJ (2000) Bacterial respiration: a flexible process for a changing environment. Microbiology 146:551–571

Schröder I, Johnson E, de Vries S (2003) Microbial ferric iron reductases. FEMS Microbiol Rev 27:427–447

Suzuki I (2001) Microbial leaching of metals from sulfide minerals. Biotechnol Adv 19:119–132

Thomas PE, Ryan D, Levin W (1976) An improved staining procedure for the detection of the peroxidase activity of cytochrome P-450 on sodium dodecyl sulfate polyacrylamide gels. Anal Biochem 75:168–176

Tolkatchev D, Yu L, Yu CA (1996) Potential induced redox reactions in mitochondrial and bacterial cytochrome b-c_1 complexes. J Biol Chem 271:12356–12363

Tyson GW et al (2004) Community structure and metabolism through reconstruction of microbial genomes from the environment. Nature 428:37–43

Walt A, Kahn ML (2002) The *fixA* and *fixB* genes are necessary for anaerobic carnitine reduction in *Escherichia coli*. J Bacteriol 184:4044–4047